Interfacial Instability Triggered Coulomb Crystallization of Charged Water Droplets

Sanjay V. Kulkarni* and Abhijit Sen†

Institute for Plasma Research, Bhat, Gandhinagar 382428, India
(Received 2 September 2003; published 29 June 2004)

We present experimental observations of two-dimensional macroscopic Coulomb crystals of charged water droplets created on the surface of a thin layer of mineral oil that covers a volume of deionized water. The crystallization process is triggered by an electrohydrodynamic instability of the oil-water interface induced in the system by the simultaneous application of a corona discharge and a dc voltage bias. The experimental scale sizes of the observed crystals agree well with quantitative theoretical estimates of the interfacial instability. Our experiment also provides a novel and simple method for creating long-lived ordered patterns that can serve as excellent systems for basic studies of strongly coupled matter with potentially interesting applications.

The study of Coulomb crystals is an active and current area of research in a number of different branches of physics including atomic and molecular physics [1], soft condensed matter [2], and plasma physics [3]. These organized structures are convenient systems for the investigation of basic issues related to strongly coupled matter with a variety of applications [4]. Detailed knowledge about their evolution dynamics and information on the collective modes of the crystals can also provide valuable insights for understanding fundamental questions related to dynamical pattern formation in driven nonequilibrium systems. Coulomb crystals are formed when the average Coulomb energy in a system of charged particles exceeds the average thermal energy by a certain amount. The ratio of these two energies is quantified by the Coulomb coupling parameter, defined as $\Gamma = Q^2/(4\pi\epsilon_0 k_B T \Delta)$, where Q is the charge on a single particle, ϵ_0 is the vacuum permitivity, T is the temperature, k_B is the Boltzmann constant, and Δ is the average distance of separation between the particles. When $\Gamma \gg 1$ the system is said to be in the strongly coupled Coulomb (SCC) regime. In the presence of a confining field an SCC system can display a rich variety of collective behavior including transition to a crystalline state when Γ exceeds a critical value. One of the key questions of interest in the study of transition phenomena is the underlying physical process triggering the crystallization process. A variety of physical mechanisms have been identified in the past. In colloidal systems, for example, order is induced by shear flows, optical gradients, or electrophoretic forces. In clouds of trapped ions, crystallization occurs when laser cooling reduces the ion temperature to a very low value. When micron sized dust particles are immersed in an electron-ion plasma, the dust particles acquire a large amount of charge, and if the dust temperature is reduced through collisions with a background neutral gas a dust crystal can emerge. In addition to cooling the charged particles, one also needs to spatially confine them in order for the crystals to form. Confinement is usually obtained through the use of suitable electromagnetic field traps,

often in a high vacuum environment. One of the most commonly employed electromagnetic traps is the Paul trap, which is traditionally used to trap ion clouds but in more recent experiments has also been used to confine a Coulomb crystal of charged oil drops [5].

In this Letter, we present experimental observations on the evolution and formation of macroscopic two-dimensional Coulomb crystals of charged water droplets on the surface of a thin layer of mineral oil. The oil layer initially covers a volume of deionized water and the whole system is subjected to a corona discharge and a dc voltage bias. By a controlled increase of the applied voltages an instability is triggered in the system, which sets off a dynamical process that results in the creation and charging of water droplets on the surface of the oil layer. We identify the instability as an electrohydrodynamic instability of the oil-water interface [6–8] and show that the spatial scale sizes of the patterns resulting from it agree quite well with quantitative theoretical estimates of the most unstable wavelength. The crystalline patterns of water droplets, representing the nonlinear stationary state of the system, range in size from a few millimeters to a few centimeters and display a variety of symmetries and patterns that can be selected by varying the external voltages. The entire experiment is carried out at room temperature and atmospheric pressure and without employing a conventional electromagnetic trap. The Coulomb crystals, once formed, can be maintained in a stable manner for several hours at a time.

A schematic of the experimental setup is shown in Fig. 1. A metallic cylinder (with diameter 10 cm, height 5 cm, and a transparent glass bottom) is filled with deionized water, which is topped by a thin layer (2–3 mm depth) of mineral oil. An alternating high voltage at 50 Hz frequency from a 20 kV, 200 mA ac power supply is applied to a sharp needle (with a parabolic tip of 40 μm diameter) with respect to a grounded circular electrode that is kept above the metallic cylinder with the help of an insulating support. The distance between the sharp point and the cylinder is varied between 1.5 to 3 cm. A 10 kV,
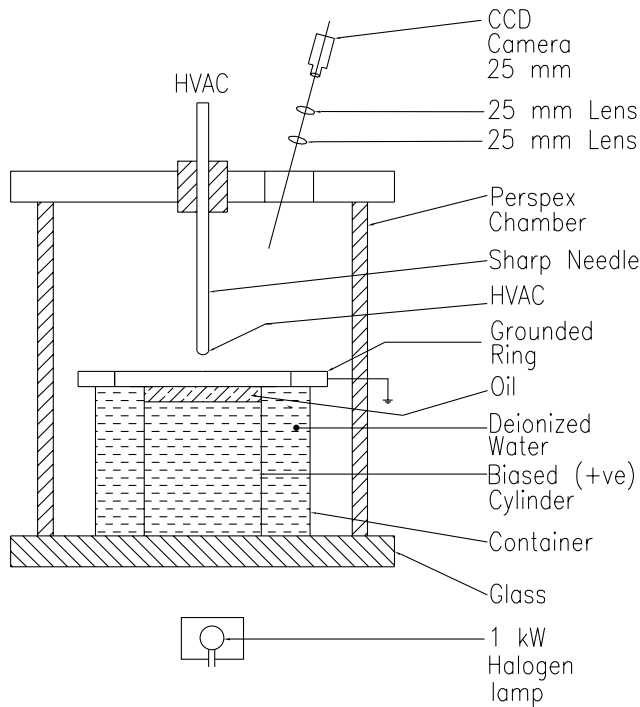
FIG. 1.   Schematic representation of the experimental setup.

100 mA high voltage dc power supply is used to positively bias the metallic cylinder with reference to a grounded central metallic circular ring. A halogen lamp fixed about 30 cm below the glass bottom of the cylinder provides proper illumination for viewing the pattern formation on the surface of oil. Care is taken to avoid any heating of the oil-water system by placing a thick perspex [Poly(methyl methacrylate) (PMMA)] slab (not shown in the figure) and a sufficient air gap between the lamp and the glass bottom. The perspex slab is additionally air cooled. The complete setup is enclosed in a perspex (PMMA) chamber to avoid airflow disturbing the structures. A charge-coupled device (CCD) camera, placed at an angle of about 20° from the vertical, is used to record the time evolution of the emerging patterns. The experiment is carried out as follows. For a fixed needle height (e.g., 1.5 cm above the oil layer) we begin by applying only the ac voltage to the system and progressively raising its value. When the ac voltage reaches a critical value (about 1.6 kV), we observe the onset of a Trichel corona discharge between the needle and the grounded ring electrode in every negative cycle of the applied voltage. The corona pulse shapes, charge, and frequency are directly confirmed on a 500 MHz oscilloscope that is connected by a 50 Ω transmission line to the grounded ring with an additional 50 Ω resistance in series. The onset voltage for Trichel pulses in our experiment is found to be practically independent of the gap between the needle and oil layer in the range of 1.5 to 3 cm. The measured value of 1.6 kV corresponds to a maximum electric field that exceeds the value of 30 kV/cm in the region near the needle tip in agreement with predicted theoretical values for avalanche buildup

[9]. As we further increase the voltage we find a threshold value at which the oil layer displays a slight rippling activity in a tiny region immediately below the needle. This threshold voltage V_{rip} is a function of the distance of the needle from the oil layer and is found to be 2.7, 3.7, 4.6, and 5.5 kV for electrode distances (d) of 1.5, 2.0, 2.5, and 3.0 cm, respectively. The threshold voltages correspond to an average electric field value of $E_{avg} = V/d \approx$ 1.8 kV/cm at the surface of the oil layer, which appears to represent the minimum electric pressure necessary to perturb the oil surface. However, this electric pressure is not sufficient to produce the droplets and the formation of crystals. For this we now turn on the dc voltage bias, keeping the ac voltage at the threshold value, and observe the enlargement of the rippling area, which appears as a white turbulent spot. In this region the oil layer appears to be pushed away and the water surface to be pulled up. The turbulent activity is accompanied by surface flows with near dipole shapes. At a certain critical size of the white spot (and a corresponding value of the total applied voltage) we observe the formation of water droplets around the poles of the dipole pattern axis. These threshold values V_{thres} of the voltage are 3, 6.5, and 8 kV for $d =$ 1.5, 2.0, and 2.5 cm, respectively. The water droplets have a spectrum of sizes and are separated at varying distances. They appear to randomly disappear or merge to form bigger size droplets that gradually move to encircle the central region. As the number of droplets increase they achieve nearly similar sizes (within about ±5% as determined from an average over many sets of measurements) and begin organizing themselves into a circular area with an inherent hexagonal symmetry among themselves. The central bubbling region slowly diminishes and disappears to give rise to a steady organized pattern of water droplets. At this point the corona discharge ceases (although the applied voltages are maintained at their original values). The entire equilibrium is extremely stable and can be observed for hours. If a drop gets accidentally destroyed or the pattern is slightly perturbed, the corona activity resumes in that local region to create additional drops and to restore the equilibrium. In Fig. 2 we show a few of the intermediate steps in the formation of the final structure of water droplets. A typical large size Coulomb crystal of water droplets is shown in the left panel of Fig. 3. The size of the structure can be controlled by varying the applied voltages. We have obtained crystals of varying sizes, including those composed of only a few droplets that resemble unit hexagonal cells (see central panel of Fig. 3) or frequently assume circular shell structures (see right panel of Fig. 3). The final size of the droplets is found to be independent of the applied voltage. The number of droplets in a crystal is found to vary linearly as a function of the applied total voltage. This is shown in Fig. 4 for three sets of observations taken for different values of the needle distance. The fitted lines (solid lines) when extrapolated to intercept the x axis give values of applied voltages that agree
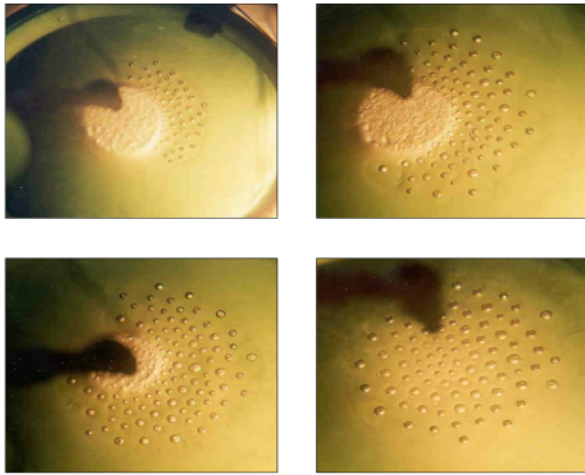
FIG. 2 (color online). Evolutionary stages of the crystal formation. The pictures are taken at intervals of a few minutes with the upper left snapshot being the earliest, followed by the upper right, the lower left, and the lower right.

with the experimentally measured threshold voltages (V_{thres}) for the onset of droplet formation. In Fig. 4 we have also shown a plot of the area of the crystal as a function of the applied voltage for one of the sets of measurements (needle distance of 2 cm). This variation too is found to be a linear function (the dashed line) of the applied voltage, implying that the area of the crystal may also be considered as an appropriate order parameter on an equal footing with the number of droplets in a crystal.

The physical mechanism responsible for the formation of the patterns appears to be a two-step process. The corona discharge charges the oil surface negatively primarily from the deposition of negative ions created in the air due to the energetic electrons emitted from the sharp tip. The free oil surface thereby acts as a virtual electrode and with the application of the dc bias induces a strong electric field in the liquid. The electric field renders the oil-water interfacial layer unstable giving rise to electro-hydrodynamic activity that is observed in the initial stages of the experiment. The basic instability arises from the interplay of two opposing forces—the stabilizing influence of the interfacial surface tension and the destabilizing effect of the electric field that tends to draw the water surface upwards in a rippled fashion. A characteristic scale length of this linear instability can be theoretically estimated [8,10] by taking a ratio of the Laplace pressure to the electrostatic pressure and is given by $\lambda_{max} = \epsilon_0(\epsilon_2 - \epsilon_1)^2 U^2/(\gamma_{12}\epsilon_1^{1/2}\epsilon_2^{1/2})$, where λ_{max} is
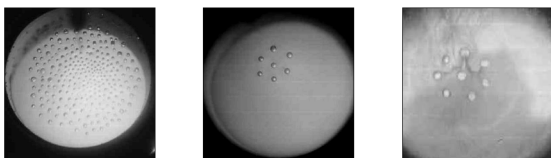
the wavelength of the fastest growing mode, ϵ_1 and ϵ_2 are the dielectric constants of mineral oil and water, respectively, γ_{12} is the interfacial tension of oil against water, and U is the applied potential difference across the oil layer. In our experiment we have $\epsilon_1 = 4.0$, $\epsilon_2 = 80.0$, $\gamma_{12} = 23$ dynes/cm, and $U \approx 102$ V, which gives us $\lambda_{max} \approx 10^{-3}$ m. This value is in good agreement with the observed spatial scale lengths of the average distances between the water droplets in the crystalline patterns. We should mention that the linear stage of the instability is characterized by the presence of a large number of scale lengths since there is a wide spectrum of unstable wavelengths. This accounts for the turbulent appearance of the initial unstable region. Eventually the wavelength, which has the maximum growth rate (denoted as λ_{max}), outgrows the other wavelengths leading to the establishment of a basic scale length for the nonlinear phase. So the process of disappearance or the merging of droplets in the initial stages can be attributed to a transient phenomenon representing the superposition of various unstable wavelengths. The formation of the pattern itself, usually with a hexagonal symmetry, can be attributed to a Coulomb crystallization process by considering the crests of the unstable water layer, which have risen to the surface of the oil layer, to behave as charged macroscopic water droplets. The mutual Coulomb repulsion of the droplets is opposed by the confining forces of the background oil surface as well as the radial component of the equilibrium electric field between the needle and the ring electrode. A quantitative measure of the electric charge Q on each droplet can be obtained by making use of the linear variation of the number of droplets with the applied voltage. Since the droplets are nearly of uniform size, we can therefore estimate Q to be $C(V/N)$ where C is the capacitance of the system (which we measure independently), V

FIG. 3. Typical large scale crystal (left) and a few droplet formations (middle and right).
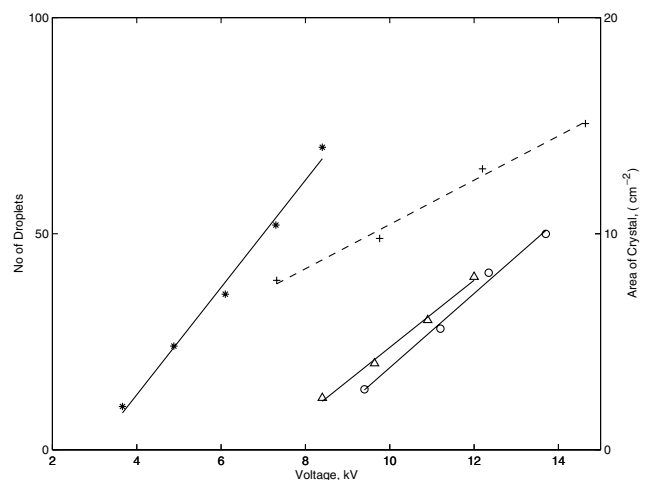

FIG. 4. Plots of number of droplets in a crystal (left ordinate, fitted solid lines) and area of the crystal (right ordinate, fitted dashed line) as a function of the applied voltage. The data sets are for different electrode spacings, namely, 1.5 cm (*), 2 cm ($\triangle$ and +), and 2.5 cm ($\bigcirc$).

is the voltage, and N is the number of droplets in the equilibrium structure. The average charge is found to be about $10^5 e$ per droplet where e is the charge of an electron. Assuming the random kinetic energy of the droplets to be that corresponding to the room temperature, we find that the Coulomb parameter $\Gamma > 10^6$, and hence the system, is in the strongly coupled regime. Thus all conditions for the formation of Coulomb crystals appear to be satisfied and to be consistent with our observations. The most common symmetry pattern we observe in the crystal is the hexagonal one but for formations with a fewer number (N) of droplets we also observe a variety of concentric shell patterns that are analogous to those observed earlier in two-dimensional molecular dynamic simulations [11] and subsequently investigated in dusty plasma configurations [12]. The control parameters are the applied voltages and the oil layer thickness that offer a direct and simple means of generating different nonlinear patterns. We have also experimented with different fluids replacing the mineral oil with other dielectric liquids and found similar results with interesting variations in the dynamical evolution of the patterns. A detailed report on these results will be given elsewhere.

In conclusion, we have experimentally delineated the dynamical processes underlying the formation of large scale two-dimensional Coulomb crystals in a simple bifluid system consisting of a thin layer of oil resting on a volume of deionized water. The crystal formation process gets initiated when external dc and ac voltages applied to the system exceed a critical value. While the entire evolutionary process is quite complex, we are able to identify some of the principal stages and contributory factors. The triggering mechanism is an electrohydrodynamic instability of the oil-water interface that forces water droplets to appear at the surface of the oil layer. The corona discharge contributes towards the accumulation of large amounts of charge on these droplets and the corresponding rise in the Coulomb coupling parameter. A direct measurement of the charge confirms that the system of droplets is indeed in the strongly coupled regime. The spatial scale lengths (lattice spacing) of the crystals are in good quantitative agreement with the theoretically estimated values of the most unstable wavelength of the linear interfacial instability. The symmetry and sizes of the crystals depend on the bias voltages and are easily controllable. The crystals can also be maintained stably for several hours. In this regard, it is worth pointing out that, in addition to providing an insight into the symmetry breaking instability that triggers pattern formation, our experiment offers a simple and novel way of creating macroscale and long-lived Coulomb crystals in the laboratory. The experimental findings also reveal some interesting dynamical observations that merit future investigation. The constancy of the size of the droplets and the agreement of the basic scale length of the interdroplet distance with linear instability lengths are somewhat surprising and need to be better understood from a fully nonlinear dynamical point of view. Our experimental technique can be usefully employed for a variety of such future investigations involving nonlinear studies of interfacial instabilities, collective excitations in strongly coupled matter, and controlled studies of phase transitions in driven nonequilibrium systems.

———————

*Electronic address: kulkarni@ipr.res.in
†Electronic address: abhijit@ipr.res.in

[1] M. Drewsen et al., Phys. Rev. Lett. **81**, 2878 (1998); W. M. Itano et al., Science **279**, 686 (1998); T. Mitchell et al., Science **282**, 1290 (1999); T. Schatz, U. Schramm, and D. Habs, Nature (London) **412**, 717 (2001); N. Kjærgaard and M. Drewsen, Phys. Rev. Lett. **91**, 095002 (2003); M. Drewsen et al., J. Phys. B **36**, 525 (2003).

[2] C. A. Murray and D. G. Grier, Annu. Rev. Phys. Chem. **47**, 421 (1996); W. K. Kegel and A. van Blaaderen, Science **287**, 290 (2000); E. R. Weeks et al., Science **287**, 627 (2000); M. Megens and W. L. Vos, Phys. Rev. Lett. **86**, 4855 (2001).

[3] G. E. Morfill et al., Phys. Rev. Lett. **83**, 1598 (1999); M. Zuzic et al., Phys. Rev. Lett. **85**, 4064 (2000); S. Nunomura, D. Samsonov, and J. Goree, Phys. Rev. Lett. **84**, 5141 (2000); T. Misawa et al., Phys. Rev. Lett. **86**, 1219 (2001); V. Nosenko, J. Goree, Z. W. Ma, and A. Piel, Phys. Rev. Lett. **88**, 135001 (2002); G. Joyce, M. Lampe, and G. Ganguli, Phys. Rev. Lett. **88**, 095006 (2002).

[4] C. Hollenstein, Plasma Phys. Controlled Fusion **42**, R93 (2000); B. M. Jelenkovic et al., New Directions in Antimatter Chemistry and Physics, edited by C. M. Surko and F. Gian-turco (Kluwer Academic, The Netherlands, 2001), Chap. 1; J. N. Tan, J. J. Bollinger, and D. J. Wineland, IEEE Trans. Instrum. Meas. **44**, 144 (1995); J. J. Bollinger et al., Phys. Rev. Lett. **63**, 1031 (1989); T. Baba and I. Waki, Jpn. J. Appl. Phys. **35**, L1134 (1996); M. A. van Eijkelenborg, M. E. M. Storkey, D. M. Segal, and R. C. Thompson, Phys. Rev. A **60**, 3903 (1999); K. Molhave and M. Drewsen, Phys. Rev. A **62**, 011401(R) (2000); G. Selwyn, J. Singh, and R. Bennett, J. Vac. Sci. Technol. A **7**, 2758 (1989).

[5] M. Triplett, R. Younger, and S. Robertson, in Physics of Dusty Plasmas, AIP Conf. Proc. No. 446 (AIP, New York, 1998), 265; S. Robertson and R. Younger, Am. J. Phys. **67**, 310 (1999).

[6] J. Reynolds, Phys. Fluids **8**, 161 (1965).

[7] L. Gor'kov and D. Chernikova, JETP Lett. **18**, 68 (1973).

[8] Z. Lin et al., J. Chem. Phys. **114**, 2377 (2001).

[9] E. Kuffel and W. S. Zaengle, High-Voltage Engineering (Pergamon Press, New York, 1984).

[10] E. Schaffer, T. Thurn-Albrecht, T. P. Russell, and U. Steiner, Nature (London) **403**, 874 (2000).

[11] H. Totsuji, T. Kishimoto, and C. Totsuji, Phys. Rev. Lett. **78**, 3113 (1997).

[12] W. Juan et al., Phys. Rev. E **58**, R6947 (1998).